

# Generic TECS based autopilot for an electric high altitude solar powered aircraft

Nir Kastner, Gertjan Looye

**Abstract** High altitude long endurance UAVs draw increasing attention in recent years. Combined with solar electrical power, they can be expected, for example, to complement the role of stationary satellites as inexpensive alternatives. This paper discusses the approach used in designing a full featured TECS (Total Energy Control System) based generic autopilot for conducting long-endurance autonomous missions with the ELHASPA (ELectric High Altitude Solar Powered Aircraft) platform and the progress made to date.

## 1 Introduction

ELHASPA (Fig.1) is a product of collaboration between DLR, EADS-astrium, EADS-Cassidian and SFL GmbH to produce a concept demonstrator for an electric high altitude solar powered platform. Featuring a wingspan of 23 m and weighing at around 100 kg, it is designed to carry a small payload to altitudes ranging at 15 to 20 km. Built entirely out of composite materials, ELHASPA is characterized by an extremely flexible structure. Overall design and structure dictate a very limited flight speed regime of between 7 and 12 m/s.

Being a long endurance mission oriented autonomous platform, operating within tight airspeed constraints and prone to frequent limitation violation, a TECS based flight control system FCS proved a natural choice for ELHASPA. This was greatly

---

Nir Kastner

German Aerospace Center (DLR), Robotics and Mechatronics Center, Institute of System Dynamics and Control, Münchner Straße 20, D-82234 Oberpfaffenhofen-Weßling, e-mail: Nir.Kastner@dlr.de

Gertjan Looye

German Aerospace Center (DLR), Robotics and Mechatronics Center, Institute of System Dynamics and Control, Münchner Straße 20, D-82234 Oberpfaffenhofen-Weßling, e-mail: Gertjan.Looye@dlr.de

motivated by TECS's flexibility, allowing for autopilot features and protection mechanisms to be integrated. Another motivating factor was the remaining uncertainties in the aerodynamic and engine models due to lack of experimental data at this early stage of the project and the significant aeroelastic effects expected. This dictated a less model-dependent choice for the FCS than for example nonlinear dynamic inversion NDI. TECS has been demonstrated to provide good platform independent coordination for longitudinal control [8], [2]. Former experience gathered at DLR with TECS includes the REAL program [2] and ATTAS (Fig.1) flight tests.

The objective of this paper is to outline a way in which TECS may be implemented into a full featured generic autopilot architecture, supporting all expected flight modes and addressing all protection and mode transition aspects. Also presented is the progress made to date with the ELHASPA project.

First, the ELHASPA demonstrator shall be presented, followed by an examination of the generic autopilot architecture which has been developed and a look at some of the simulation analysis and flight test results for both ATTAS and ELHASPA. Finally, future progress approach shall be discussed.



**Fig. 1** Left - ELHASPA demonstrator, Right - ATTAS DLR research platform

## 2 The ELHASPA platform

ELHASPA has a twin-boom high aspect-ratio configuration. Available control surfaces comprise of two ailerons, fitted each at the outward most wing sections, two monoblock elevators and two monoblock rudders, located aft on each boom. For structural considerations, the ailerons have only limited travel and control effectiveness. Propulsion is electric regenerative, with solar panels covering most of the wing's upper surface. The two nacelle house the two electromotors with constant-pitch propellers, batteries and electronics. The sensor suit comprises of two pitot tubes, located mid-wing between the nacelle, GPS and IRU units. All sensor com-

ponents are doubled for redundancy reasons.

The aircraft has been modeled through an integrated modeling approach, making use of the Modelica language [6] and the DLR Flight Dynamics Library [5]. In its full extent, it features six degrees of freedom flight dynamics, aeroelastic effects and an energy system module. Aerodynamics were derived using the vortex lattice method. Mass and stiffness properties were obtained from measurements and computer-aided design data. Propulsion was attained from measurements and modeling. For simulation, both rigid and elastic model derivatives are available. Factors have been extensively built in into the model for the purpose of supporting an uncertainty analysis as part of the design process. For further details please refer to [4].

### 3 The TECS control law

First introduced by [1], TECS is a conventional alternative control law for the longitudinal flight control system of an aircraft. Let the total energy of an aircraft be:

$$E = E_{POT} + E_{KIN} = Wh + WV^2/2g \quad (1)$$

The momentary total energy feed rate is therefor:

$$\dot{E} = \dot{E}_{POT} + \dot{E}_{KIN} = W\dot{h} + WV\dot{V}/g \quad \text{with:} \quad \dot{h} = V\sin(\gamma) \cong V\gamma \quad (2)$$

$$\Rightarrow \dot{E} \cong WV(\gamma + \dot{V}/g) \quad (3)$$

One defines the specific total energy feed rate as:

$$\Rightarrow \dot{E}_S \equiv \dot{E}/WV \cong \gamma + \dot{V}/g \equiv \dot{E}_{S_{POT}} + \dot{E}_{S_{KIN}} \quad (4)$$

An approximation for the required thrust yields:

$$W\dot{V}/g \cong T - D - W\sin(\gamma) \cong T - D - W\gamma \Rightarrow (T - D)/W \cong \gamma + \dot{V}/g \equiv \dot{E}_S \quad (5)$$

That is, the momentary specific total energy feed rate  $\dot{E}_S$  required in order to maintain the combination of current specific kinetic energy feed rate  $\dot{E}_{S_{KIN}} \equiv \dot{V}/g$  and current specific potential energy feed rate  $\dot{E}_{S_{POT}} \equiv \gamma$  is proportional to the current available thrust.

An airspeed or mach number command may be converted to represent a specific kinetic energy feed rate command  $\dot{E}_{S_{KINc}}$  (i.e. **"KIN target"**).

A flight path angle, rate of climb or altitude command may be converted to represent a potential specific energy feed rate command  $\dot{E}_{S_{POTc}}$  (i.e. **"POT target"**).

Under the assumption that required thrust changes are dominant over the changes in drag  $\Delta T \gg \Delta D$ , the error between the commanded and current specific total energy feed rate is:

$$\Delta \dot{E}_S = \Delta \dot{E}_{SPOT} + \Delta \dot{E}_{SKIN} = (\dot{E}_{SPOT_c} - \dot{E}_{SPOT}) + (\dot{E}_{SKIN_c} - \dot{E}_{SKIN}) \quad (6)$$

$$= (\gamma_c - \gamma) + (\dot{V}_c - \dot{V})/g = (\Delta T_c - \Delta D)/W \cong \Delta T_c/W \quad (7)$$

This allows for a control law to be conceived which would govern a commanded momentary specific total energy feed rate  $\dot{E}_{S_c}$  to the system. The control law consist of the  $K_{EI}$  gain scaled command error integration term and the  $K_{EP}$  gain scaled proportional feedback damping term.

$$\Delta T_c/W = \Delta \dot{E}_S \cdot K_{EI} \cdot \frac{1}{S} - \dot{E}_S \cdot K_{EP} \quad (8)$$

Flight path angle adjustment, through elevator movement for instance, transfer specific potential energy feed rate  $\dot{E}_{SPOT}$  into kinetic energy feed rate  $\dot{E}_{SKIN}$  and vice versa, practically without loss. In analogy to the specific total energy feed rate term  $\dot{E}_S$ , one defines the specific energy distribution feed rate  $\dot{D}_S$ :

$$\dot{D}_S \equiv -\dot{E}_{SPOT} + \dot{E}_{SKIN} = -\gamma + \dot{V}/g \quad (9)$$

$$\Rightarrow \Delta \dot{D}_S = \dot{D}_{S_c} - \dot{D}_S = (-\dot{E}_{SPOT_c} + \dot{E}_{SKIN_c}) - (-\dot{E}_{SPOT} + \dot{E}_{SKIN}) \quad (10)$$

$$= -(\gamma_c - \gamma) + (\dot{V}_c - \dot{V})/g \propto \Delta \delta_{e_c} \quad (11)$$

A second control law is derived for the commanded momentary specific total energy distribution feed rate command  $\dot{D}_{S_c}$ :

$$\Delta \delta_{e_c} \propto \Delta \dot{D}_S \cdot K_{DI} \cdot \frac{1}{S} - \dot{D}_S \cdot K_{DP} \quad (12)$$

## 4 Autopilot architecture

Fig.2 depicts a classical hierarchical structure for a flight control system FCS with autopilot AP. Raw signals from the aircraft sensors are processed and passed on, together with other system inputs, to the different downstream FCS components. The FCS inner loop IL, also known as stability augmentation system SAS, modifies the aircraft's characteristic handling qualities to the designer's specification. The FCS outer loop OL translates high end autopilot mode commands (i.e. path and airspeed tracking) to FCS inner loop inputs. An autopilot logic unit APL is a state machine, which manages the transition between the autopilot flight modes, thus supporting flight mission plan capabilities. A flight mission plan may be executed by the pilot through consecutive manual mode selection on the autopilot panel APP, or managed by the flight management system computer FMS.

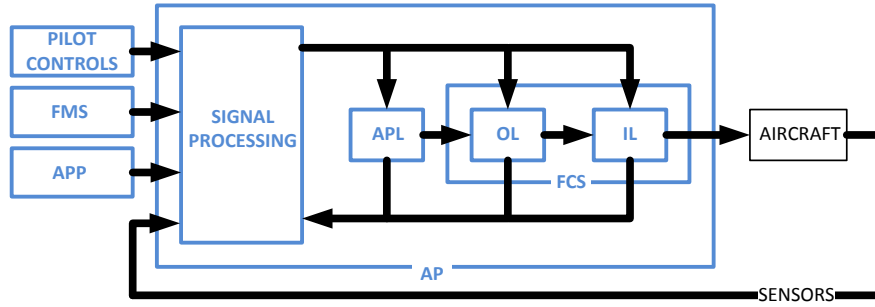


**Fig. 2** Classical hierarchical structure for a flight control system with autopilot

**Choice of FCS inner loop:** The lack of experimental aerodynamic data, confirming the analytical model, introduced a degree of model uncertainty to the early phase of the project. In the absence of an experimentally validated model, the choice was made to initially avoid a FCS inner loop altogether and rely on the inherent longitudinal and lateral static stability incorporated into the basic design. TECS is particularly suited for this purpose, with the original design [1] commanding thrust and elevator directly without an inner loop.

**FCS outer loop and TECS architecture:** Path tracking outer loop architecture is, with the exception of TECS, conventional and to large extent inherited from REAL [2]. This includes the gain setting which may be considered platform independent. The TECS controller belongs inside the FCS outer loop block (Fig.2), translating "high-end" path and airspeed tracking commands into FCS inner loop command inputs. The following discussion should help in depicting a way of effectively integrating TECS into a full featured autopilot architecture.

The TECS control law is reformulated in equations (13), (14). It differs from the classical standalone TECS layout [1] in the order of integration and the breakdown into "TECS prestige" and "TECS core".

$${}^{\text{TECS core}} = \begin{cases} \Delta T_c / W = (\Delta \dot{E}_S \cdot K_{EI} - \dot{E}_S \cdot K_{EP} \cdot S) \cdot \frac{1}{S} \\ \Delta \delta_{ec} \propto (\Delta \dot{D}_S \cdot K_{DI} - \dot{D}_S \cdot K_{DP} \cdot S) \cdot \frac{1}{S} \end{cases} \quad (13)$$

$${}^{\text{TECS prestige}} = \begin{cases} \Delta \dot{E}_S = (\gamma_c - \gamma) + (\dot{V}_c - \dot{V}) \cdot \frac{1}{g} \\ \dot{E}_S = \gamma + \dot{V} \cdot \frac{1}{g} \\ \Delta \dot{D}_S = -(\gamma_c - \gamma) + (\dot{V}_c - \dot{V}) \cdot \frac{1}{g} \\ \dot{D}_S = -\gamma + \dot{V} \cdot \frac{1}{g} \end{cases} \quad (14)$$

The change in integration order inside the "TECS core" (Fig.3) creates a single integration path, thus simplifying the introduction of the two integrator windup mechanisms for thrust and pitch-associated limitations. Once at limit, the integration

of a TECS path is halted and an integrator windup mechanism ensures a command value marginally outside the commandable limit. As soon as the corresponding  $\Delta \dot{E}_S$  or  $\Delta \dot{D}_S$  command term takes on a tendency away from the triggered saturation, normal path integration is commenced, decimating the margin  $\varepsilon$  and leading to a controlled exit out of windup. This TECS representation also eliminates the need to consider any initial values, otherwise necessary in order to guarantee that the damping feed-back terms  $\dot{E}_S$  and  $\dot{D}_S$  be equal to zero at the moment the TECS core is engaged.

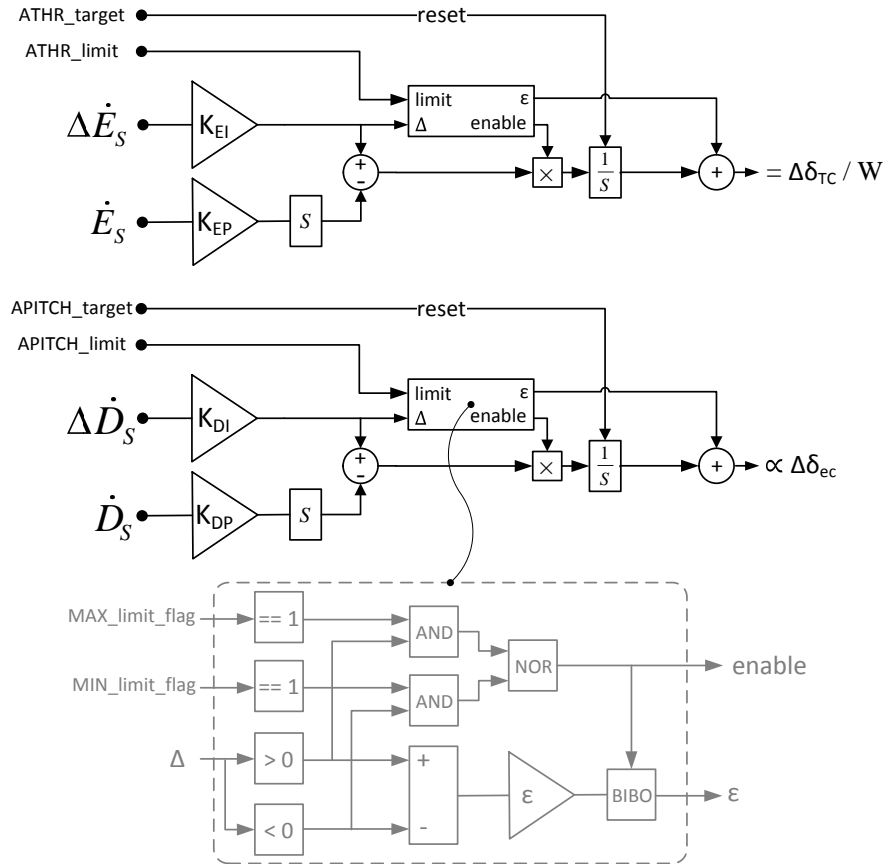


**Fig. 3** TECS core

The breakdown into "TECS prestige" (Fig.4) and "TECS core" (Fig.3) reflects the reformulated TECS control law (13), (14). Also evident from this layout is the distinctive uncoupled nature of the TECS paths.

At this stage, a terminology shall be adopted, which would be used in this paper. For simplicity, and keeping with the TECS concept, the flight control of an aircraft in the vertical plain can be viewed as a system with two outputs - thrust command  $T_c$  (i.e. auto-throttle **"ATHR"**) and elevator command  $\delta_c$  (i.e. auto-pitch **"APITCH"**) and two inputs - kinetic and potential specific energy feed rate commands  $\dot{E}_{SKIN_c} \equiv \dot{V}_c/g$  (i.e. **"KIN target"**) and  $\dot{E}_{SPOT_c} \equiv \gamma_c$  (i.e. **"POT target"**).

The term **"dual"** shall therefore be used to relate to a maneuver for which a **"KIN target"** and a **"POT target"** are to be pursued simultaneously, with both thrust (**"ATHR"**) and elevator (**"APITCH"**) allocated for the FCS as command outputs.

Should either thrust or elevator be deprived as command output for the FCS, aircraft flight dynamics dictate that an airspeed associated command be controlled either by pitch alone, while thrust is set by the pilot (i.e. **"KIN by APITCH"**), or by thrust alone, with the aircraft's pitch attitude determined by the pilot (i.e. **"KIN by ATHR"**).

Providing that sufficient thrust is available, a flight path angle associated command may be controlled by pitch alone (i.e. **"POT by APITCH"**), but for all practical reasons, not by thrust alone.

The **"SPD/FPA Priority-Control"** TECS feature [1] is used in its original context only in conjunction with the **"dual"** autopilot mode. The **"Priority-Control"** concept is also what allows TECS to operate in the **"SPD by APITCH"** and **"POT by APITCH"** autopilot modes. The **"damping boost"** TECS feature (see {2-K;K} gains [1]), affecting the  $\dot{D}_S$  damping term (13) has been retained and must be treated for safe case-dependent limits when operating in the **"SPD by APITCH"** and **"POT by APITCH"** autopilot modes (see  $\dot{D}_S$  path Fig.4) . For consistency, the TECS **"SPD/FPA Priority-Control"** and the **"damping boost"** TECS features shall be referred to as **"KIN/POT Priority-Control"** and **"KIN/POT damping boost"** respectively.

Inside the **"TECS prestage"** (Fig.4) the four input terms to the **"TECS core"** -  $\Delta\dot{E}_S$ ,  $\dot{E}_S$ ,  $\Delta\dot{D}_S$ ,  $\dot{D}_S$  are managed. Two upper autopilot logic unit signals - **"ATHR target"** and **"APITCH target"** take on the values **"dual"**, **"KIN"**, **"POT"** and **"none"**, defining the switching between the flight mechanic modes - **"dual"**, **"KIN by ATHR"**, **"KIN by APITCH"** and **"POT by APITCH"**. Note that  $\Delta\dot{E}_S$  and  $\Delta\dot{D}_S$  are being integrated inside the **"TECS core"** and  $\dot{E}_S$  is continuous by nature. Therefore only the  $\dot{D}_S$  term is treated for discontinuities resulting from switching (see **"Blend In Blend Out"** BIBO filter).

**Interaction between TECS and autopilot logic unit:** The above terminology proved very instrumental in conceiving an autopilot logic unit. In the same manner a favorable base transformation may reduce a complex set of equations into a much

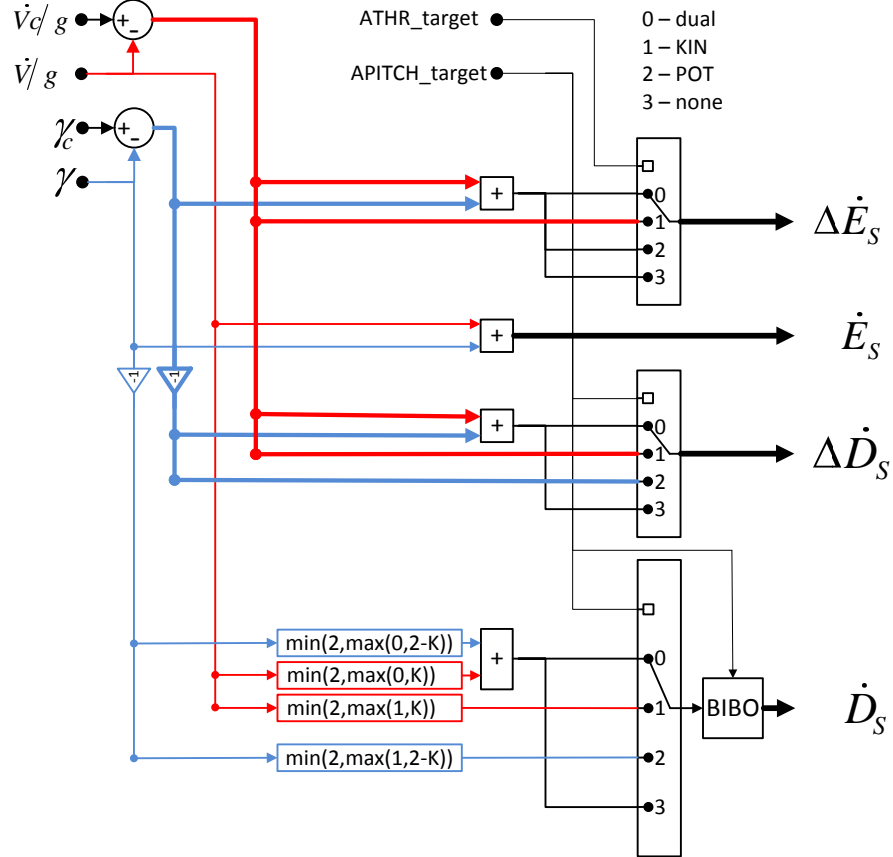


**Fig. 4** TECS prestage

more compact form, a convenient choice of signal terminology inside the autopilot logic unit allows for a very efficient formulation, avoiding a significantly more complex state machine.

Inspired by TECS, high-level FMS oriented autopilot flight mode terminology (i.e.: SPD/M, VS/FPA, FLCH, HDG, TRK, GS, LOC etc.) is re-associated into the flight-mechanic oriented terminology (i.e.: "dual", "KIN by ATHR", "KIN by APITCH" and "POT by APITCH") discussed above. Notice that while thrust limitation needs to be considered inside the autopilot logic unit, pitch-associated limitation needs not. With thrust in limit, while in "dual" mode, one of either current "KIN target" or "POT target" must be pursued while the other sacrificed. No such parallel applies to pitch-associated limitation, as there exist no practical "POT by ATHR" flight mode.



## 5 ATTAS simulation analysis

The generic autopilot has been subjected to extensive analysis tests. These included both ELHASPA dedicated simulations, as well as simulations conducted within the scope of ATTAS flight tests and various analysis. Much commonality exists between the generic autopilot versions used for both ATTAS and ELHASPA. Due to the early stage of the ELHASPA program, simulation analysis and flight test results will concentrate on the experience gathered with ATTAS. The DLR Flight Dynamics Library [5] served as a simulation environment. It includes realistic atmosphere, wind, turbulence and sensor modeling. For the purpose of this presentation, the turbulence effects were turned off, so that the characteristic behavior may be observed.

For ATTAS, a  $\{\Theta_c, \Phi_c, \Psi_c\}$  following NDI based inner loop has been married to the generic autopilot architecture. TECS has been configured to operate with "POT Priority-Control" (while in dual mode) and "POT damping boost" ( $K = 2$ ). As mentioned before, inner and outer loop controller paths and gain settings were to large extent inherited from REAL [2]. The simulation concentrated therefor upon proving the correct operation of the different autopilot mode transition and protection mechanisms which integrate the already proven inherited control path components into a full featured autopilot concept. The simulation scenarios brought here were carefully chosen so that some practical aspects could be discussed which are relevant to autopilot design.

**"KIN by APITCH" simulation analysis:** The simulated behavior for the KIN by APITCH flight mode is presented in Fig.5. A common practice flight mode, motivated by the requirement to operate at constant engine setting, prolonging engine life expectancy. Beginning with a "dual" airspeed and altitude hold, a "KIN by APITCH" climb is performed, ending with a "dual" airspeed and altitude hold level-off.

To see is the function of the theta command authority feature. Its purpose is to restrict the range of pitch attitude which TECS is allowed to command for the inner loop to follow. Unrestricted, TECS would command a nose-down/up attitude corresponding to an acceleration/deceleration command. Complementing common features such as  $\dot{V}_c$  limiter and speed command shaping, the theta command authority feature restricts pitch commands such, that an acceleration/deceleration be pursued with a nose-down/up attitude change not exceeding a predetermined authority range. This range is determined relative to the current pitch attitude captured at the moment the airspeed command has been changed, while remaining climb/descent associated (i.e. non-negative/non-positive vertical speed), whichever the less restricting. In this way, FCS behavior remains predicable and intuitive for the pilot. That is for example, speed changes during climb do not result in momentary steep descent. Notice the closing and opening theta command authority windows, allowing TECS to operate unrestricted as much as possible and how the lower limit changes from being "pitch attitude change" to "positive rate of climb" related. This information is presented to the pilot on the primary flight display PFD (Fig.6) along with an

"increase/decrease thrust" message respectively. A pilot induced throttle change in accordance with these directions, triggers the opening up of the currently enforced limitation.

The theta command authority introduces an artificial pitch-associated FCS limitation, extending the already existing elevator-travel limit windup protection feature, protecting the  $\Delta\dot{D}_S$  TECS command path the same way the  $\Delta\dot{E}_S$  command path is being protected against thrust-associated integrator windup (Fig.3). The ATTAS  $\{\Theta_c, \Phi_c, \Psi_c\}$  following NDI based inner loop does not have a  $\Theta_c$  integrator term. This meant that a stationary  $\Theta_c$  following error had to be taken into account.

One potentially dangerous scenario which needs to be addressed in this context is the transition from climb into descent while conducting a climb. Since the theta command authority feature involves capturing the current pitch attitude as a reference, a transition from climb to descent would see (if not addressed correctly) the autopilot trying to accelerate from climb to descent speed around a climb associated pitch attitude, while reducing throttle from climb to descent power. This would lead to stall. For this reason the current pitch attitude is to be successively recaptured as long as the throttle position is changing from climb to descent power, resulting in a slow shifting-along of the theta command authority window until settling around a descent associated pitch attitude.

**"dual" simulation analysis:** Fig.7 show an analysis for a "dual" climb scenario. Starting with a "dual" airspeed and altitude hold", a "dual" airspeed and flight path angle hold climb is performed, ending with a "dual" airspeed and altitude capture and hold level-off. The commanded speed and flight path angle combinations were carefully chosen such, that the thrust limitation integrator windup protection and recovery could be tested. Especially interesting is the unattainable combination  $\{90[m/s]; 4^\circ\}$ . The "POT Priority-Control" configuration for the TECS controller, means that while operating in "dual" mode with thrust currently at limit, only one command may be pursued while the other sacrificed. A decision has been taken to always prioritize the "POT target" over the "KIN target" (here flight path angle over airspeed). This philosophy assumes that a pilot would prefer the intuitive task of monitoring his airspeed, while expecting the autopilot to hold the commanded trajectory. This holds especially for an approach maneuver, where trajectory deviation would be perceived as disorienting. Eventual airspeed violation is prevented by the speed protection feature. Current autopilot mode and limitation information is relayed to the pilot over the primary flight display and auto pilot panel. Fig.8 shows the auto pilot panel captured during the simulated scenario discussed above. In center of the panel are the three "FCS actuators" - APITCH, ATHR and ALAT ("auto lateral") symbolically depicted as stick and throttle quadrant. Color coding helps indicate whether an "actuator" is under pilot (gray) or autopilot (shades of green) control. Should an autopilot allocated "actuator" be at limit, the corresponding "actuator" symbol and currently sacrificed command turn from solid to blinking green (depicted here in yellow).

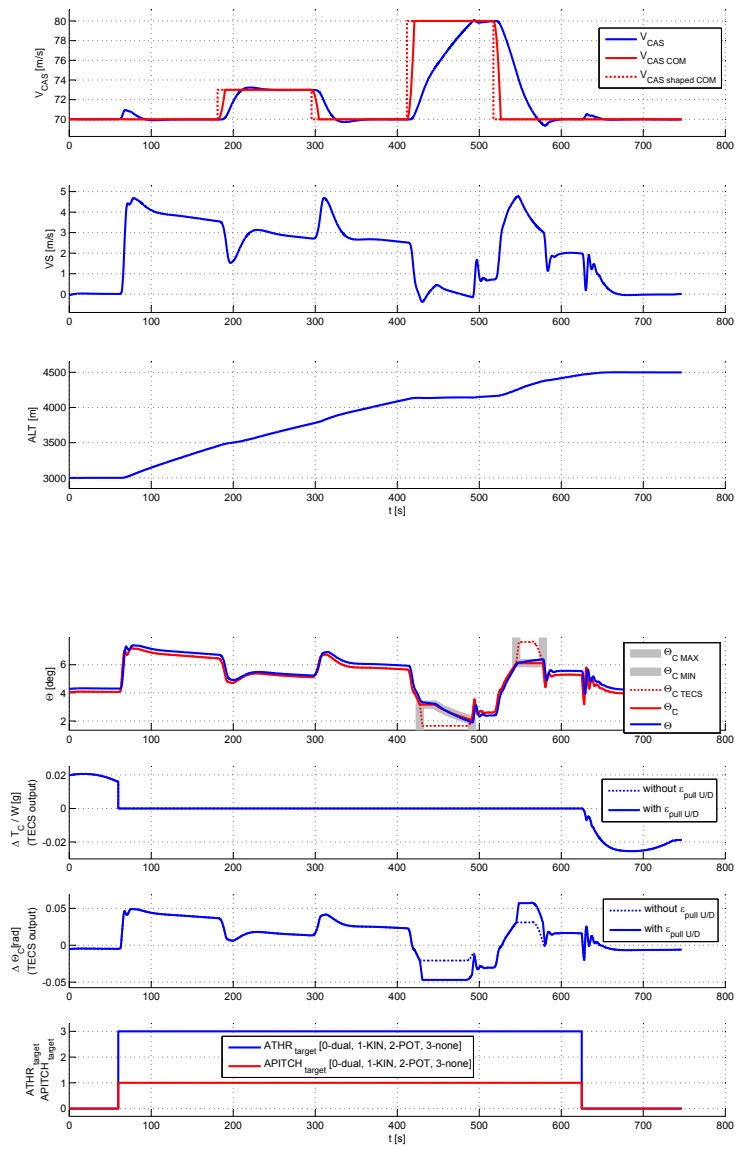


**Fig. 5** ATTAS simulation analysis - KIN by APITCH climb scenario

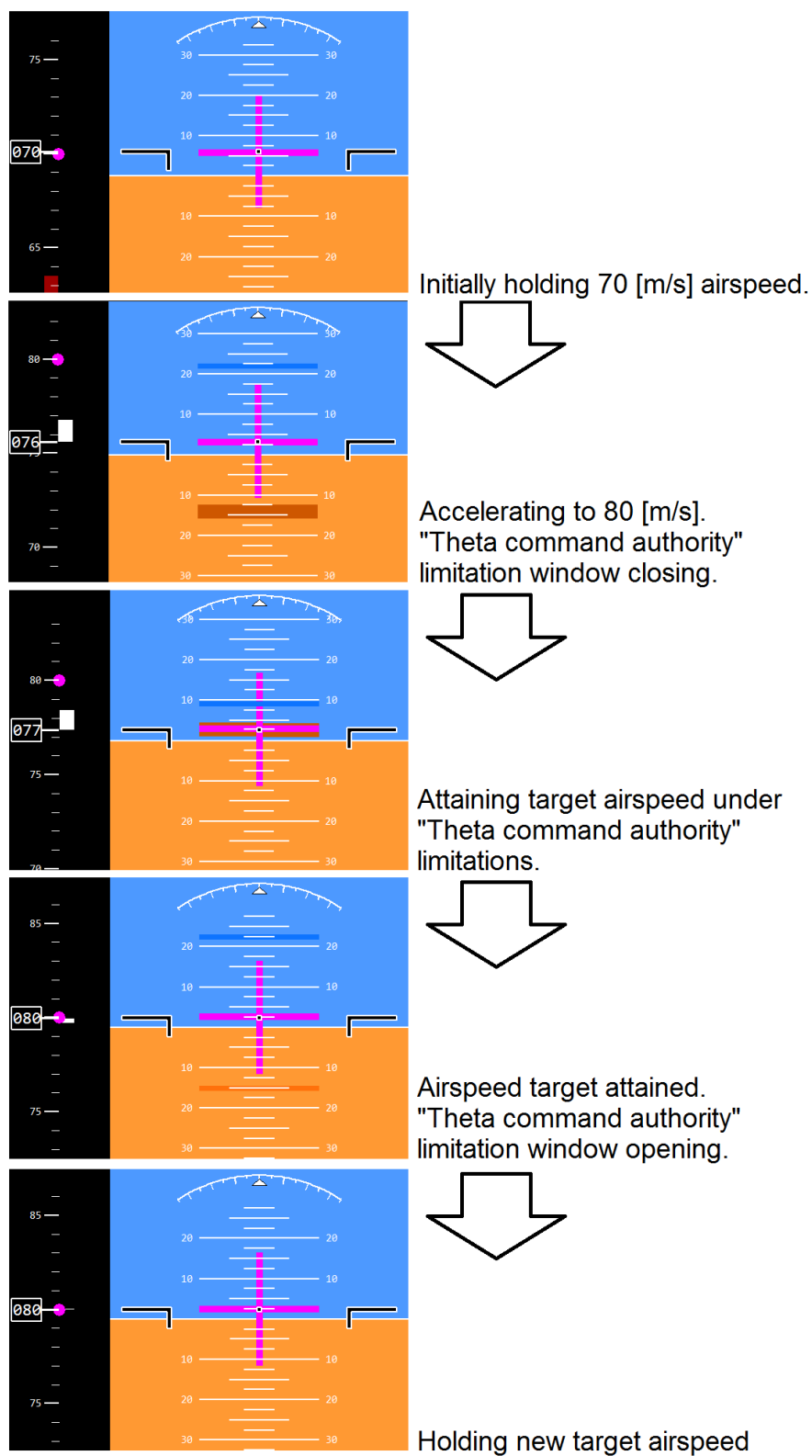


**Fig. 6** ATTAS simulation analysis - KIN by APITCH climb scenario - PFD representation of theta command authority limitation feature

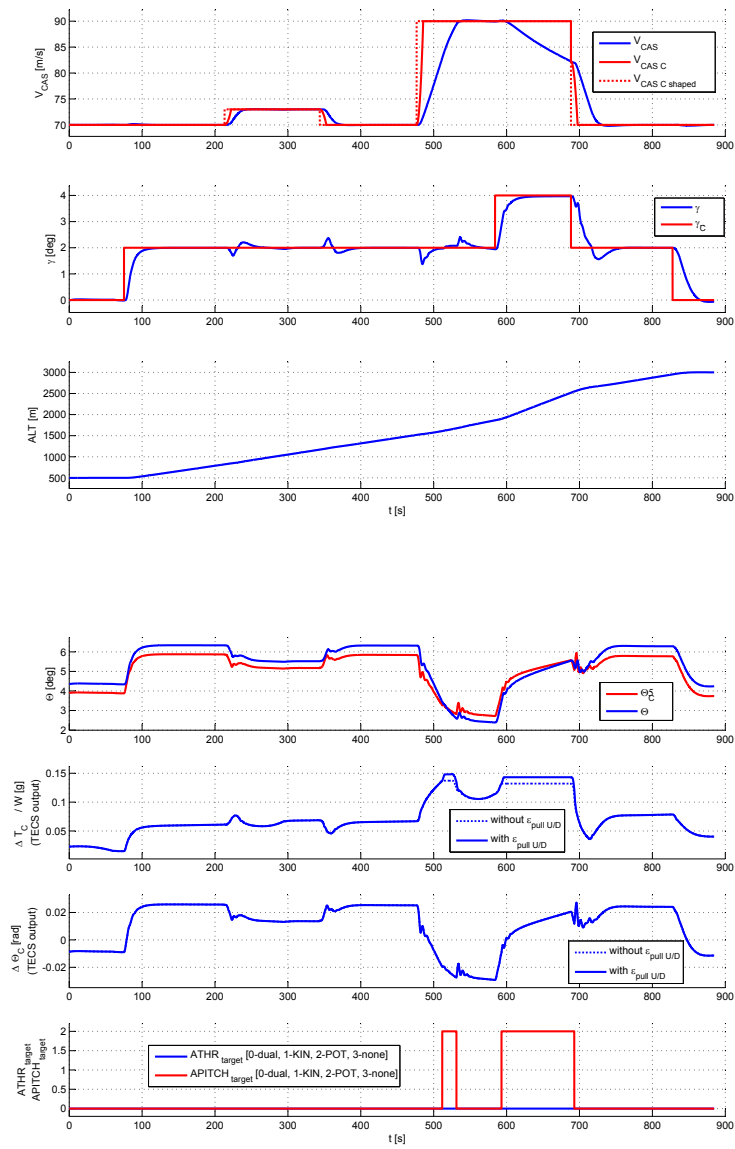


**Fig. 7** ATTAS simulation analysis - dual climb scenario

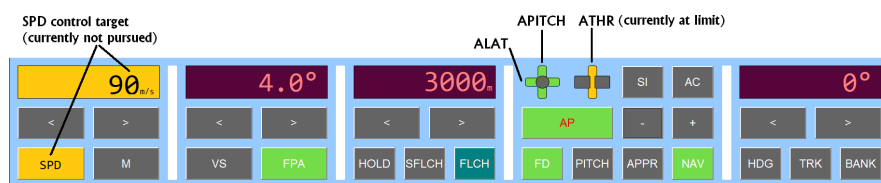


**Fig. 8** ATTAS simulation analysis - dual climb scenario - thrust limitation representation on Auto Pilot Panel (APP)

Much experience has been gathered with the generic autopilot while conducting monte-carlo analysis for an ATTAS automatic landing flare-laws investigation, within the scope of another project, which shall be the subject of a future publication. This and other analysis proved to be very instrumental in testing the correct function and reliability of all non-classical control theory autopilot components (i.e. logics, protection/limitation features etc.).

## 6 ATTAS Flight test results

Presented here are some of the maneuvers which were tested with the ATTAS platform in flight. The flight test program included: "dual" climb/descent, "KIN by APITCH" climb/descent, "KIN by ATHR" climb/descent and "energy exchange". Lateral autopilot standard modes such as: heading, track and bank angle hold were tested as well. Also, the performance of vertical and lateral FCS working together was tested in flight, performing a trajectory following "helix descent" maneuver [3].

Fig.9 depicts a "KIN by APITCH" climb. Different airspeed steps were commanded while throttle was kept constant at climb power throughout the climb. The function of the theta command authority feature, discussed above, may be observed. Notice that the somewhat disappointing characteristic oscillatory pitch command response is due to the ATTAS elevator auto-trim mechanism which operates autonomously from the FCS and interfered throughout the flight with the proper action of the FCS. The relatively short setting time allowed after each command step was due to air traffic control constraints, which given the busy test flight program, had to be kept to a minimum. These apply to all ATTAS flight test results presented in this paper.

The results for an "energy exchange" maneuver are presented in Fig.10. Airspeed and Altitude changes were commanded simultaneously and calculated such, that no energy change should result. That is, the increase in kinetic energy equals the potential energy loss and vice versa. The aim was to observe to what extent the TECS thrust command would remain unaffected. During an energy exchange maneuver,

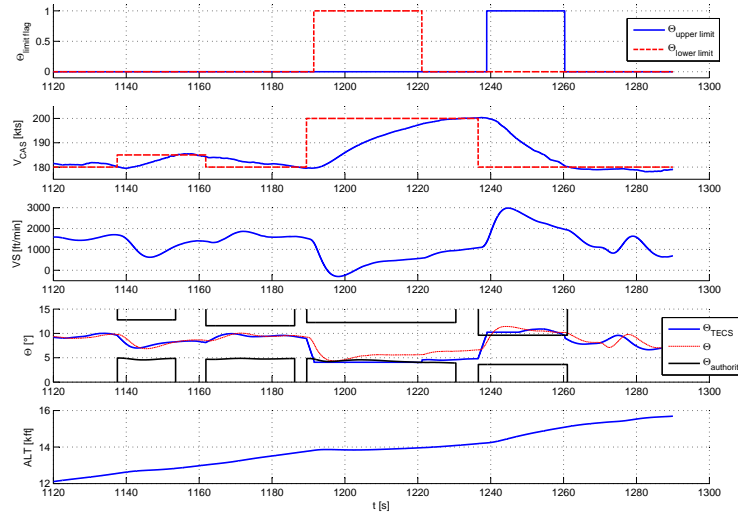


**Fig. 9** ATTAS flight test results - KIN by APITCH climb scenario

TECS should theoretically command no thrust change, providing that the airspeed and altitude control path gains are balanced, which was not the case for ATTAS. As can be seen, the TECS thrust command activity has been characteristically moderate, with some of the activity owing to the elevator auto-trim mechanism.

The longitudinal and lateral tracking performance for a trajectory following helix maneuver are presented in Fig. 11. Originally conceived for an acoustic noise reduction non-standard approach trajectory capability requirement [3], this maneuver is representative for the trajectory following flight mode of the generic autopilot. In this mode the flight management system FMS computes the following continuous guidance command streams for the FCS to follow:  $\{V_c, h_c, \gamma_c\}$  in the longitudinal plain and  $\{\Delta y, \chi_c, \psi_c\}$  in the lateral plain. This constitutes a current angular deviation and translatory deviation guidance command pair for both plains. Note that an additional  $\psi_c$  command is required for the lateral guidance in order to account for trajectory curvature, which is not necessary for the vertical guidance. As can be seen, satisfactorily position deviations in the order of  $\pm 10$  [m] were attained. Speed changes during the maneuver did not affect the tracking performance.

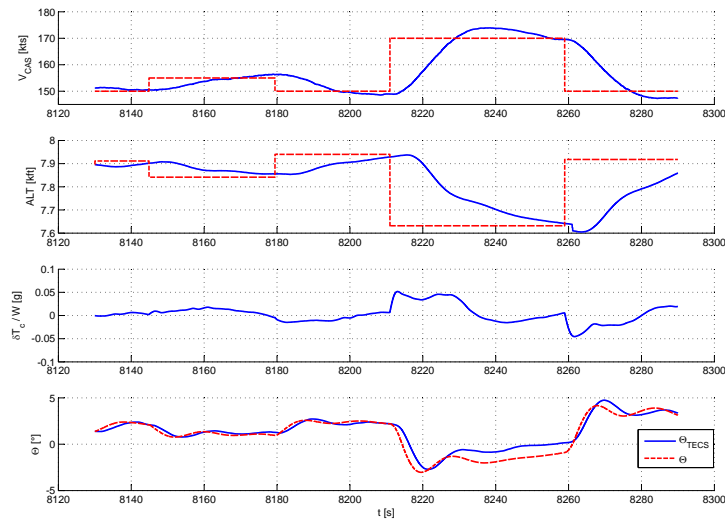


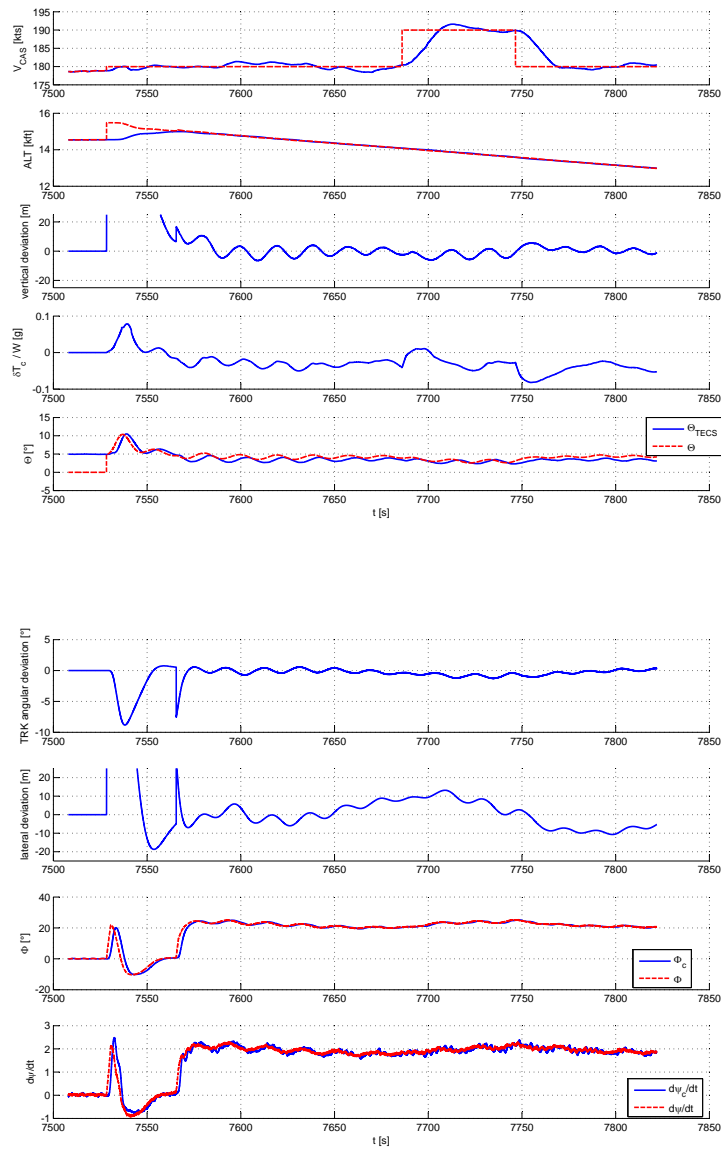
**Fig. 10** ATTAS flight test results - energy exchange scenario

## 7 ELHASPA Simulation analysis

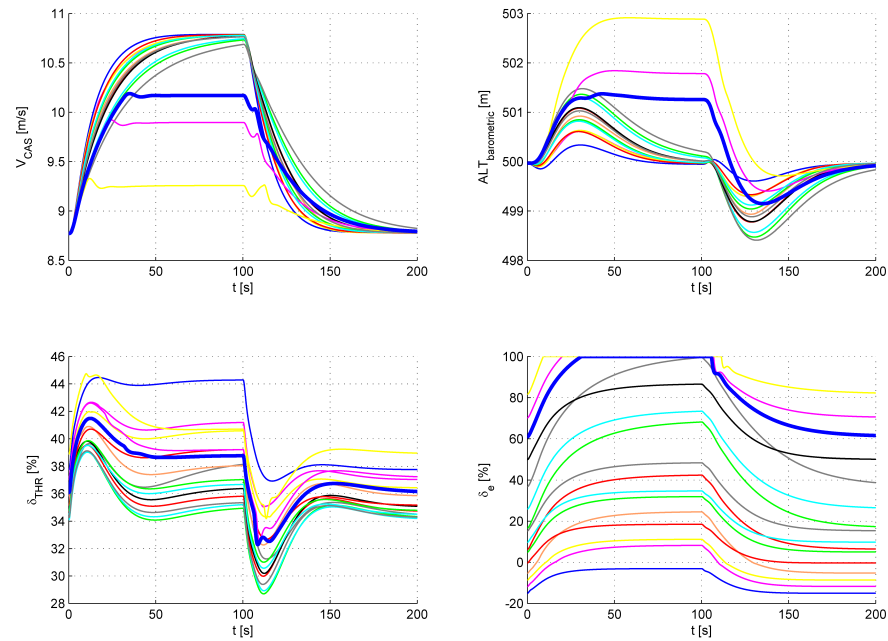
For ELHASPA robustness analysis, the multi-objective optimization-based software environment for control system design MOPS [7] was used. In the example brought here, the basic design assumption of inherent static stability for the longitudinal plain has been validated by a MOPS analysis prior to confirmation in manual flight tests. The analysis saw the variation of all relevant aerodynamic coefficients within an uncertainty range of  $\pm 30\%$  while demonstrating stability and/or safe operation of the respective triggered FCS limitation protection mechanisms.

Fig.12 depicts an analysis for one such a criterion. Here, a speed step - altitude hold maneuver was performed. One concern was that not sufficient "nose down" elevator travel exists for the maiden flight configuration. As can be seen here, for most of the uncertainty parameter combinations, sufficient control authority is available and the maneuver is successfully executed. For those combinations, for which this is not the case, safe elevator saturation windup and recovery operation could be demonstrated. That is, if elevator travel limitation has been reached, airspeed and altitude have been maintained until an attainable airspeed was commanded.





**Fig. 11** ATTAS flight test results - trajectory following "helix descent" scenario



**Fig. 12** ELHASPA simulation analysis - dual airspeed step altitude hold robustness analysis example

## 8 ELHASPA Flight test results

First ELHASPA manual flight test results have confirmed the basic design assumption of inherent static stability, thus making possible the gradual introduction of the autopilot in its current architecture into operation. The next step would see the extending of the FCS to include an inner loop, as soon as a validated model be made available for gain optimization analysis. The decision would fall for a minimal inner loop architecture that would provide an improvement of handling characteristics in manual fly by wire FCS mode, increased path following performance in autopilot FCS mode and allow for additional useful features to be integrated, which require an inner loop, such as theta command authority. Already during the first manual flight tests, room for improvements could be identified, calling for a "rate-command-attitude-hold" manual fly by wire FCS in order to reduce pilot workload during landing and improve touchdown point precision and speed control for the longitudinal plain. Also, adverse yaw could be observed in the lateral plain. The improvement of turn characteristics shall be the focus of the coming flight tests [4].

## 9 Conclusion

A full featured TECS based generic autopilot was developed. The design has successfully undergone initial flight testing on-board the ATTAS research platform for proof of concept. TECS has proven very compatible, allowing for all expected autopilot features to be addressed and promising with regard to FCS performance. The basic design is to be used for the ELHASPA demonstrator, where it is intended to provide autonomous mission capabilities. Further ELHASPA model validation is required prior to adoption of a final FCS inner loop architecture and gain optimization analysis.

## References

1. A. A. Lambregts. vertical flight path and speed control autopilot design using total energy principles, AIAA paper 83-2239, 1983.
2. Gertjan H.N. Looye, An Integrated Approach to Aircraft Modelling and Flight Control Law Design. PhD thesis, Delft University of Technology 2007.
3. Gertjan H.N. Looye (2011) Helical Flight Path Trajectories for Autopilot Evaluation. In: Selected Papers of the First CEAS Specialist Conference on Guidance, Navigation and Control Advances in Aerospace, Guidance, Navigation and Control. Springer. Seiten 79-90. ISBN 978-3-642-19816-8.
4. Andreas Klöckner, Daniel Schlabe, Gertjan Looye, Martin Leitner. Integrated Modelling of an Unmanned High-Altitude Solar-Powered Aircraft for Control Law Design Analysis, (*paper currently in revision*) CEAS EuroGNC 2013
5. Gertjan Looye. The new DLR flight dynamics library. Proceedings of the 6th International Modelica Conference, vol 1, pp 193-202, 2008.
6. Fritzson P (2004) Principles of object-oriented modeling and simulation with Modelica 2.1. Wiley-IEEE Press.
7. Hans-Dieter Joos, Johan Bals, Gertjan Looye, Klaus Schnepfer, Andreas Varga. A multi-objective optimisation-based Software environment for control system design (MOPS). Proceedings, IEEE International
8. Boeing Condor UAV (<http://www.boeing.com/history/boeing/condor.html>).

## Nomenclature

KIN - kinetic (i.e. kinetic specific energy feed rate)  
 POT - potential (i.e. potential specific energy feed rate)  
 TECS - Total Energy Control System  
 NDI - nonlinear dynamic inversion  
 IL - inner loop  
 OL - outer loop  
 FCS - flight control system  
 SPD - speed

FPA - flight path angle  
 VS - vertical speed  
 FLCH - flight level change  
 HDG - heading  
 TRK - track (course)  
 BANK - bank angle  
 AP - autopilot  
 APL - autopilot logic unit  
 APITCH - auto-pitch  
 ATHR - auto-throttle  
 ALAT - auto-lateral  
 FMS - flight management system  
 PFD - Primary Flight Display  
 BIBO - Blend In Blend Out filter  
 GPS - Global Positioning System  
 IRU - Inertial Reference Unit  
 $\Delta$  - general notation for "commanded - current value" deviation  
 $g$  - earth gravity [ $\text{m/s}^2$ ]  
 $W$  - weight [N]  
 $T, T_c$  - thrust (command) [N]  
 $\delta_{THR}$  - absolute throttle position [%]  
 $\delta_e$  - absolute elevator deflection [%]  
 $V_{CAS}$  - calibrated airspeed [m/s]  
 $V, V_c$  - general notation for airspeed (command) [m/s]  
 $\dot{V}, \dot{V}_c$  - general notation for airspeed derivative (command) [ $\text{m/s}^2$ ]  
 $h$  - general notation for altitude [m]  
 $\dot{h}$  - general notation for altitude derivative [m/s]  
 $\gamma, \gamma_c$  - flight path angle (command) [rad]  
 $\Theta, \Theta_c$  - pitch attitude (euler) angle (command) [rad]  
 $\Phi, \Phi_c$  - roll attitude (euler) angle (command) [rad]  
 $\dot{\Psi}, \dot{\Psi}_c$  - heading change rate (command) [rad/s]  
 $E, E_{KIN}, E_{POT}$  - total/kinetic/potential energy [J]  
 $\dot{E}, \dot{E}_{KIN}, \dot{E}_{POT}$  - total/kinetic/potential energy derivative [J/s]  
 $\dot{E}_{SKIN}, \dot{E}_{SKIN_c}$  - specific kinetic energy feed rate (command) "KIN target" [rad]  
 $\dot{E}_{SPOT}, \dot{E}_{SPOT_c}$  - potential specific energy feed rate (command) "POT target" [rad]  
 $\dot{E}_S, \dot{E}_{S_c}, \dot{D}_S, \dot{D}_{S_c}$  - total/distribution specific energy feed rate (command) [rad]  
 $K_{EI}, K_{EP}, K_{DI}, K_{DP}$  - TECS control law integration and proportional terms gains  
 $K$  - TECS control law "KIN/POT damping boost" gain